Relevance of the Materno-Fetal Interface for the Induction of Antigen-Specific Immune Tolerance

Angelina Mimoun, Sandrine Delignat, Ivan Peyron, Victoria Daventure, Maxime Lecerf, Jordan Dimitrov, Srinivas Kaveri, Jagadeesh Bayry, Sébastien Lacroix-Desmazes

journal of
thrombosis and haemostasis

Transplacental delivery of therapeutic proteins by engineered IgG: a step towards perinatal replacement therapy

Journal:	*Journal of Thrombosis and Haemostasis*
Manuscript ID	JTH-2023-00001.R1
Article Type:	Original Article
Date Submitted by the Author:	n/a
Complete List of Authors:	Mimoun, Angelina; Centre de Recherche des Cordeliers, Equipe 16 INSERM UMRS 1138 Bou Jaoudeh, Melissa; Centre de Recherche des Cordeliers, Equipe 16 INSERM UMRS 1138 Delignat, Sandrine; Centre de Recherche des Cordeliers, Equipe 16 INSERM UMRS 1138 Daventure, Victoria; Centre de Recherche des Cordeliers, Equipe 16 INSERM UMRS 1138 Reyes Ruiz, Alejandra; Centre de Recherche des Cordeliers, Equipe 16 INSERM UMRS 1138 Lecerf, Maxime; Centre de Recherche des Cordeliers, Equipe 16 INSERM UMRS 1138 Azam, Aurélien; Centre de Recherche des Cordeliers, Equipe 16 INSERM UMRS 1138 Noe, Remi; Centre de Recherche des Cordeliers, Equipe 16 INSERM UMRS 1138 Peyron, Ivan; INSERM, U1176 HITh; INSERM U1176 Christophe, Olivier; INSERM , U1176 Lenting, Peter J.; INSERM, 1176 Proulle, Valerie; APHP, Service Hematologie Biologique et UF Hemostase Clinique, Hopital Cochin, APHP. Universite de Paris; INSERM, INSERM UMRS 1138 McIntosh, Jenny; UCL Cancer Institute, Deparment of Haematology Nathwani, Amit; University College of London Cancer Institute, Haematology Dimitrov, Jordan; Centre de Recherche des Cordeliers, Equipe 16 INSERM UMRS 1138 Denis, Cécile; INSERM, Unit 1176 Lacroix-Desmazes, Sebastien; Centre de Recherche des Cordeliers, Equipe 16 INSERM UMRS 1138
Key Words:	hemophilia A, Factor VIII, transplacental delivery, neonatal Fc receptor, engineered antibodies

Title. Transplacental delivery of therapeutic proteins by engineered IgG: a step towards perinatal replacement therapy

Authors. Angelina Mimoun,* Melissa Bou Jaoudeh,* Sandrine Delignat,* Victoria Daventure,* Alejandra Reyes Ruiz,* Maxime Lecerf,* Aurélien Azam,* Remi Noe,* Ivan Peyron,† Olivier D Christophe,† Peter J Lenting,† Valérie Proulle,*,‡ Jenny McIntosh,§ Amit C Nathwani,§,¶ Jordan D Dimitrov,* Cécile V Denis,† Sébastien Lacroix-Desmazes*

Affiliations. *Institut National de la Santé et de la Recherche Médicale, Centre de Recherche des Cordeliers, CNRS, Sorbonne Université, Université de Paris, F-75006 Paris, France; †Laboratory for Hemostasis, Inflammation & Thrombosis, Unité Mixed de Recherche 1176, Institut National de la Santé et de la Recherche Médicale, Université Paris-Saclay, 94276 Le Kremlin-Bicêtre, France; ‡Service d'Hématologie Biologique, Hôpital Cochin, AP-HP.Centre, Paris, France; §Deparment of Haematology, UCL- Cancer Institute, London, United Kingdom; ¶Katherine Dormandy Haemophilia and Thrombosis Unit, Royal Free London NHS Foundation Trust, London, United Kingdom.

Running heads. Transplacental delivery of protein therapeutics

Correspondence should be addressed to Sébastien Lacroix-Desmazes (Sebastien.Lacroix-Desmazes@crc.jussieu.fr). INSERM UMRS 1138, Centre de Recherche des Cordeliers 15, rue de l'école de médecine, 75006 Paris - France

Word count. 4930 words; 4 figures; 1 supplementary file

Abstract (239 words)

Background: Transplacental delivery of maternal IgG provides humoral protection during the first months of life until the newborn's immune system reaches maturity. The materno-fetal interface has been exploited therapeutically to replace missing enzymes in the fetus, as shown in experimental mucopolysaccharidoses, or to shape adaptive immune repertoires during fetal development and induce tolerance to self-antigens or immunogenic therapeutic molecules.

Objective: To investigate whether proteins that are administered to pregnant mice or endogenously present in their circulation may be delivered through the placenta.

Methods: We engineered monovalent IgG (FabFc) specific for different domains of human factor VIII (FVIII), a therapeutically relevant model antigen. The FabFc were injected with exogenous FVIII to pregnant severe hemophilia A mice or to pregnant mice expressing human FVIII following AAV8-mediated gene therapy. FabFc and FVIII were detected in the pregnant mice and/or fetuses by ELISA and immunohistochemistry.

Results: Administration of FabFc to pregnant mice mediated the materno-fetal delivery of FVIII in a FcRn-dependent manner. FVIII antigen levels achieved in the fetuses represented 10% of normal plasma levels in the human. We identify antigen/FabFc complex stability, antigen size and shielding of promiscuous protein patches, as key parameters to foster optimal antigen delivery.

Conclusions: Our results pave the way towards the development of novel strategies for the *in utero* delivery of endogenous maternal proteins to replace genetically deficient fetal proteins or to educate the immune system and favor active immune tolerance upon protein encounter later in life.

Keywords: hemophilia A, factor VIII, transplacental delivery, neonatal Fc receptor

Introduction

The placenta forms a privileged interface between the mother and the fetus; it excretes wastes (urea, carbon dioxide...) from fetal circulation and supplies fetus with nutrients, water and oxygen that are vital for its growth [1]. The placenta also mediates the active transfer of maternal immunoglobulin G (IgG). Maternally transferred IgG protect the newborn against a broad spectrum of pathogens until the immune system is mature enough to produce its own IgG. Conversely, the transplacental delivery of maternal IgG may be deleterious to the fetus when the antibodies are specific for self-molecules [2][3][4]. The transcytosis of maternal IgG initiates with their non-specific fluid phase internalization by syncytiotrophoblasts [5,6]. Internalized IgG accumulate in early endosomes and bind to the neonatal Fc receptor (FcRn) upon acidification of the endosome content [7]. IgG/FcRn complexes then reach the basal pole of the cells; IgG are released from the FcRn in the intercellular space following fusion of the sorting endosomes with the cell membrane and return to neutral pH [8]. In humans, IgG transfer starts during the second half of the second trimester of pregnancy [9,10]. In rodents, a weak but non-negligible transfer of maternal IgG is detected from day 15 of gestation (E15) and peaks at E17; maternal IgG are however mainly transferred via lactation after birth through the intestinal epithelium [11–13].

The FcRn-mediated transplacental delivery of molecules can be exploited for therapeutic purposes. Vaccination of pregnant women elicits protective IgG that are transferred to the fetuses and protects the newborns against flu, diphtheria, pertussis, pneumonia or SARS-Cov2 [14,15]. The *in utero* therapeutic replacement of missing lysosomal enzymes was achieved in a mucopolysaccharidosis VII pre-clinical model, where the Fc-fused beta-glucuronidase injected to pregnant mice crossed the placenta, reached the fetal circulation and restored lysosomal digestion of accumulated proteins [16]. Fc-fused proteins administered to pregnant mice also shape the immune system of the offspring following transplacental delivery.

Transplacentally delivered proteins thus alter the T-cell repertoire of the offspring [17] and elicit antigen-specific regulatory T cells that are protective again antigen challenge [18] or development of spontaneous autoimmunity [19] later in life. We hypothesized that native proteins administered to pregnant mice or endogenously present in their circulation may be deliberately delivered to the fetus through the placenta for therapeutic purposes.

Using human factor VIII (FVIII) as a therapeutically relevant model antigen, and engineered monovalent anti-FVIII IgG (FabFc), we show that exogenous FVIII was delivered from the mother circulation to that of the fetuses upon binding to anti-FVIII FabFc, at protein levels that corresponded to 10% of the normal FVIII plasma levels in the human. The transfer of FVIII required binding of the FabFc to the FcRn. Binding of FabFc to the mother's FcγRs only remotely influenced the FabFc-mediated transplacental delivery of FVIII. We finally identified stability of the antigen/antibody complex, size of the antigen and shielding of promiscuous protein patches on the FVIII light chain as key parameters to foster optimal protein delivery, thus paving the way towards the development of *in utero* replacement therapy and induction of active specific immune tolerance.

Materials and Methods (also see supplemental material online)

Production of FVIII-specific FabFc

BOIIB2, KM33 and BO2C11 FabFc were derived from anti-FVIII IgG isolated from hemophilia A (HA) patients [20–22]. cDNA encoding the variable region (V) genes of the light chains were cloned in plasmids encoding the constant human kappa light chain, by In-fusion® cloning (Takara Bio, Shiga Prefecture, Japan). cDNA encoding the variable region (V) genes of the heavy (H) were cloned in plasmids encoding the constant heavy chain of human Fcγ1 separated from a second constant heavy chain of human Fcγ1 by a $(GGGS)_4$ linker, to generate the VH-CH1-CH2-CH3-linker-CH2-CH3 polypeptide chain. The heavy and light chain-

encoding plasmids were co-transfected into non-adherent ExpiHEK human embryonic kidney cells (Thermo Scientific, Waltham, Massachusetts). Day-7 supernatants were collected and FabFcs were purified on a HiTrap™ rProtein A FF sepharose column (Cytiva, Marlborough, Massachusetts).

FVIII binding ELISA

Full-length FVIII (2.5 µg/mL, Advate®, Takeda, Osaka, Japan) was immobilized on ELISA plates (Thermo Scientific). Following blocking with PBS, 3% BSA (Sigma Aldrich, St Louis, Missouri), FabFc and IgG in blocking buffer were added to the plate. FVIII-bound IgG and FabFc were detected with a mouse anti-human IgG Fc conjugated to HRP (9040-05, Southern Biotech, Birmingham, Alabama) or with a goat anti-human Ig Fc conjugated to HRP (2047-05, Southern Biotech) and OPD substrate (Sigma Aldrich). Alternatively, FabFc and IgG (5 nM) were immobilized, plates blocked with PBS, 1% low fat milk, 0.1% tween 20, and FVIII diluted in blocking buffer. Fixed FVIII was detected using the biotinylated mouse anti-FVIII A2 domain IgG GMA8015 (Green Mountain Antibodies, Burlington, Vermont) in PBS, 3% BSA, 0.1% tween 20, streptavidin-HRP and OPD substrate. Optical densities were measured at 492 nm with a TECAN Infinite 200 (Männedorf, Switzerland). When indicated, IgG and FabFc (13 nM) were incubated in FVIII-coated plates in 20 mM Hepes, 150 mM NaCl, 2.5 mM $CaCl_2$, at pH ranging from 3 to 8, prior to revelation.

Inhibition of FVIII binding to VWF by FabFc and IgG

FabFc and IgG were pre-incubated with full-length FVIII (0.2 nM, 0.06 µg/mL, Advate®) at 37°C for 30 min in 20 mM Hepes, 150 mM NaCl, 3% BSA, and added for 1 hour at 37°C on VWF (10 µg/mL, Wilfactin®, LFB, Les Ulis, France)-coated ELISA plates. The residual VWF-bound FVIII was detected with a biotinylated mouse monoclonal GMA8015 (1 µg/mL) or with

a biotinylated mouse anti-C2 domain IgG (1 µg/mL, ESH8, Sekisui Diagnostics, Burlington, Massachusetts) prior to addition of streptavidin-HRP and TMB substrate (Thermo Scientific, Waltham, Massachusetts). Optical densities were measured at 450 nm.

Animals

Six to twelve-week old FVIII exon 16 knock-out (FVIII-KO) mice and double von Willebrand factor (VWF)/FVIII-KO mice on the C57Bl6 background were used. Animals were handled in agreement with local ethical authorities (approval by Charles Darwin ethics committee, authorizations APAFIS#8219-2016121917406953 v3 and APAFIS#30960-2021070116253589 v4).

***In vivo* AAV gene transfer and FVIII expression**

Six-week old FVIII-KO females were injected retro-orbitally with AAV8 FVIII-V3 [23] (200 µL, $2x10^{13}$ vg/kg) containing a codon-optimized BDD-FVIII transgene, diluted in PBS containing 0.025% human serum albumin. Transgenic FVIII in plasma was followed by ELISA and functional coagulation assay for 2 weeks before mating. Transgenic FVIII antigen was detected by ELISA using ESH8 (1 µg/mL) for capture and GMA8015 (1 µg/mL) for detection, streptavidin-HRP, and the TMB substrate. The pro-coagulant activity of transgenic FVIII was measured in a functional chromogenic coagulation assay (Siemens Healthcare, Erlangen, Germany). For both assays, human standard plasma (Siemens) was used as a standard. Females were mated 2 weeks following gene therapy and used for transplacental delivery experiments at E17.5 of pregnancy (i.e., within 4 to 18 weeks following mating).

Transplacental delivery of FVIII

To study the transplacental delivery of exogenous FVIII, naïve FVIII-KO pregnant mice at E17.5 were injected (200 µl in the retro-orbital vein) with different molecules: BDD-FVIII (50 µg, NovoEight®, Novo Nordisk), full-length FVIII (70 µg, Helixate®, Bayer), rFVIIIFc (50 µg, Eloctate®, Sanofi), FVIII pre-incubated with FabFc (29.1 µg) in 20 mM Hepes, 150 mM NaCl, 2.5 mM $CaCl_2$ pH7.4 for 30 min at 4°C. FabFc (29.1 µg) was also pre-incubated with the home-made recombinant C2 domain [24] of FVIII at 5.5. µg prior to injection. To study the FabFc-mediated transplacental delivery of endogenous FVIII, E17.5 FVIII-KO pregnant mice expressing transgenic FVIII following AAV gene transfer (4.1±1.9 nM, Fig 3B), were injected (200 µl in the retro-orbital vein) with 0.15, 1.5 or 4 µg FabFc. Blood was collected on citrated tubes (Greiner bio-one, Kremsmünster, Austria) from the pregnant mothers 5 min and 4 hours following injection, and from the fetuses at 4 hours, plasma was prepared and saved in aliquots at -80°C degrees until use.

Detection of FabFc in mouse plasma

Capture of native FabFc and $FabFc^{N297A}$ was achieved using a mouse anti-human IgG Fc (LS-C69574, LSbio, Seattle, Washington) and that of $FabFc^{IHH}$ was achieved by coating a goat anti-human kappa (2060-01, Southern biotech). Following incubation with mouse plasma, native FabFc and $FabFc^{N297A}$ were revealed using a mouse anti-human IgG Fc conjugated to HRP (9040-05, Southern Biotech) and $FabFc^{IHH}$ was revealed with a goat anti-human Fc Ig-HRP (2047-05, Southern Biotech). KM33 FabFc, KM33 $FabFc^{N297A}$, and KM33 $FabFc^{IHH}$, were quantified in mice plasma using the corresponding purified FabFc as standard. The optical density was measured at 492 nm after addition of the OPD substrate.

Detection of exogenous FVIII and C2 domain in mouse plasma

FVIII alone or pre-incubated with the anti-C2 domain BO2C11 or with the anti-A2 domain BOIIB2 FabFc was captured with a home-produced monoclonal human anti-FVIII C1 domain IgG (LE2E9) [25]. FVIII pre-incubated with the anti-C1 domain KM33 FabFc was captured with the human monoclonal anti-FVIII A2 domain IgG (BOIIB2). rFVIIIFc was captured with a mouse monoclonal anti-FVIII A2 domain IgG (GMA8015, Green Mountain) and a mouse monoclonal anti-C2 domain IgG (ESH8, Sekisui Diagnostics, Burlington, Massachusetts). FVIII was revealed with a biotinylated polyclonal sheep anti-FVIII antibody (SAF8C Biot, Affinity biological, Ontario, Canada), streptavidin-HRP (R&D system), and the TMB substrate (Thermo Scientific). The FVIII C2 domain was captured with a mouse monoclonal anti-FVIII C2 domain (GMA8026, Green Mountain) and was then revealed with a biotinylated monoclonal mouse anti-His tag IgG (BAM050, R&D system), streptavidin-HRP (R&D system), and the TMB substrate. Exogenous FVIII, rFVIIIFc and the C2 domain were quantified in mice plasma using BDD-FVIII (Novoeight ®), full-length FVIII (Helixate ®), rC2 (homemade) and rFVIIIFc (Eloctate ®) as standard respectively. The OD was measured at 450 nm.

Detection of FVIII and KM33 FabFc immune complexes in mouse plasma

FVIII/anti-C1 domain KM33 FabFc immune complexes were captured with a mouse anti-human IgG Fc (LS-C69574). FVIII/KM33 immune complexes were revealed with a biotinylated polyclonal sheep anti-FVIII antibody (SAF8C Biot), streptavidin-HRP, and the TMB substrate. Immune complexes were quantified in mice plasma using FVIII pre-incubated 30 min at 4°C with KM33 FabFc in equimolar ratio as standard.

Results

Monovalent IgG-mediated transplacental delivery of FVIII

Using the VH and VL genes of the human monoclonal anti-FVIII IgG KM33 [20], we generated a monovalent monoclonal anti-FVIII IgG, referred to as KM33 FabFc. KM33 FabFc possesses a single antigen-binding site and a complete Fc fragment stabilized by a linker peptide (**Fig. 1A**). Presence of a linker between the two Fc did not affect the binding of the Fc fragment to mouse FcRn (**Fig. S1**). KM33 FabFc and the original IgG bound and neutralized FVIII to same extents (**Fig. 1B**, **Table S1**). KM33 IgG is specific for FVIII C1 domain and inhibits FVIII binding to VWF. Accordingly, KM33 FabFc competed in a dose-dependent manner with VWF for FVIII binding (**Fig. 1C**).

We investigated whether KM33 FabFc mediates FVIII delivery from the circulation of pregnant mice to that of fetuses. Human recombinant B domain-deleted (BDD) FVIII was injected either alone or following pre-incubation with KM33 FabFc (1:1 molar ratio) to naïve pregnant FVIII-KO mice at day E17.5 of gestation. The dissociation constant (K_D) that characterizes the binding of KM33 IgG to FVIII is equal to 0.1 nM, with almost no dissociation *in vitro* (k_{off}=1.9x10^{-4} s^{-1}) [20]. Assuming that KM33 FabFc has a similar affinity as the complete IgG, >97% of the FVIII is expected to be bound to the FabFc at the time of injection to pregnant mice. Fetuses' plasma was obtained 4 hours following injection of the mothers. FVIII was not detected in the fetuses' plasma when it was injected alone (**Fig. 1D**). In contrast, FVIII was detected in the fetuses' plasma following co-injection with the FabFc, (**Fig. 1D**): FVIII as well as FVIII in complex with KM33 FabFc were detected in the fetuses' plasma using different ELISA setups. The circulating FVIII antigen concentration in fetuses' plasma was 0.13±0.11 nM, which represents 7-10% of the normal FVIII plasma levels in C57Bl6 mice or in the human (i.e., 1.8±0.4 nM and 1.2±0.6 nM [26], respectively).

We generated a mutant KM33 FabFc^{IHH} that bound to FVIII with a similar dose-dependency as the native KM33 FabFc (**Fig. S2A**) and demonstrated no affinity for mouse FcRn (**Table 1**). FVIII pre-incubated with KM33 FabFc^{IHH} was not delivered from mothers' circulation to that

of fetuses (**Fig. 1D**), indicating that the KM33 FabFc-mediated transplacental deliver of FVIII requires binding to the FcRn.

We engineered a KM33 FabFc^{N297A} mutant that lacks binding to mouse FcγR (**Fig. S2B**) but retains binding to FVIII and FcRn (**Fig. S2A, Table 1**). Ttransplacental delivery of KM33 FabFc^{N297A} was 2-fold greater than that of the native KM33 FabFc (**Fig. S3**, P<0.0001). In agreement, the FVIII amounts delivered by KM33 FabFc^{N297A} from the mothers to the fetuses (0.19±0.07 nM) were statistically greater than that delivered by the native KM33 FabFc (0.12±0.02 nM, P=0.0355). Because the gain in amounts of transcytosed FVIII by the FabFc^{N297A} mutant was biologically marginally and varied highly among fetuses, we used non-mutated FabFc in the rest of the study.

Stability of the FVIII/FabFc complex in the mothers' circulation

Four hours following injection to the mothers, the levels of KM33 FabFc detected in the fetuses' plasma were 20 to 60-fold greater than that of FabFc-bound FVIII or FVIII (**Fig. 1D**). The instability of the FVIII/FabFc complex in the mothers' circulation might account at least in part for the poor transplacental FVIII delivery. We therefore investigated whether the complex dissociates in the maternal circulation. We collected blood from the mothers 5 min and 4 hours following the injection of KM33 FabFc and FVIII, administered either alone or as a complex, and compared the percentages of injected molecules eliminated per hour. Values were calculated from the raw data shown in **Fig 2A**, as [C^{5min}–C^{4hr}]/[C^{5min} x time] x 100, where C^{5min} and C^{4hr} represent concentrations of molecules measured 5 minutes and 4 hours after injection, respectively, and time is equal to 4 hours. When KM33 FabFc and FVIII were co-injected, the circulating amount of FVIII decreased faster than that of the FabFc (22.6±1.2 %/hr versus 9.9±3.4 %/hr, respectively, P=0.0286). In contrast, the elimination rate of FVIII pre-incubated with KM33 FabFc was similar to that of FVIII injected alone (24.7±0.1 %/hr). Likewise, the

elimination rate of KM33 FabFc pre-incubated with FVIII did not differ from that of KM33 FabFc injected alone (7.8±5.2 %/hr, P=0.603). To test whether the dissociation of FVIII from the FabFc is responsible for its increased elimination rate, we treated pregnant mice with a commercially available Fc-fused recombinant FVIII (Eloctate®, rFVIIIFc). At the injected doses, the elimination rate of rFVIIIFc (22.5±1.4 %/hr) was identical to that of FVIII pre-incubated with KM33 FabFc (P>0.9) and was only marginally lower than that of FVIII injected alone.

Human FVIII accumulates rapidly in the spleen and liver following injection to FVIII-KO mice [27]. In agreement, FVIII pre-incubated with KM33 FabFc was detected in the spleen and liver 30 min following injection (**Fig 2B**). While some co-localization between FVIII and KM33 FabFc was evidenced, 65±68% of the FVIII signal in the liver and 95±5% of the FVIII signal in the spleen were not associated with that of KM33 FabFc. The data do not allow to decipher whether the dissociation of FVIII from KM33 FabFc occurs in the circulation or after endocytosis. Because the fusion of FVIII to the Fc fragment does not rescue FVIII from elimination, we hypothesize that the rapid elimination of FabFc-complexed FVIII is mediated by FVIII-specific receptors expressed by scavenger cells in the spleen and liver, leading to the intracellular degradation of the FVIII.

Stability of the FVIII/FabFc complex during transcytosis

The concentrations of FabFc and FVIII measured 4 hours following injection to pregnant mice demonstrated a 5-fold difference in the mothers' plasma and a 100-fold difference in the fetuses' plasma (**Fig. 2C**), indicating a further loss of FVIII upon placental crossing. The co-localization of FVIII with the syncytiotrophoblasts did not differ whether it was injected alone or in the presence of KM33 FabFc (**Fig. 2D**) or of KM33 FabFc^{IHH} (**Fig. S4**), suggesting that accumulation of FVIII in the placenta is not dependent on the FabFc and on binding to the

FcRn. The interaction of KM33 FabFc with FVIII was stable at pH as low as pH 4 (**Fig. 2E**), suggesting that the poor transcytosis of the FVIII/FabFc complex is not due to complex dissociation at the acidic pH that characterizes early endosomes. Likewise, the interaction of KM33 FabFc with FVIII was not impacted by changes in concentrations of $CaCl_2$ (0.1-100 mM) or NaCl (15.6-1000 mM) (data not shown). Interestingly, Fc-fused FVIII (rFVIIIFc) was not better transcytosed than FVIII co-incubated with KM33 FabFc (**Fig. 2F**, P<0.0001). Because KM33 FabFc was efficiently delivered to the fetuses (**Fig. S3**), the data suggest that the poor transplacental delivery of FVIII (either fused to the Fc fragment or in complex with FabFc) is due, for a large part, to retention of the FVIII moiety in syncytiotrophoblast cells.

Considering total blood volumes of 1.5 ml and 60 µl for pregnant mice and fetuses, respectively (i.e., 58.5 ml/kg) [28], the data indicate that 4±1‰ of the FVIII injected to the mothers reached the circulation of the fetuses in 4 hours.

Transplacental delivery of endogenous maternal FVIII

In our experimental setup, 90±5% of the exogenously administered FVIII (**Fig. 2A**) was eliminated from the mothers' circulation within 4 hours. We performed additional experiments wherein human FVIII is produced endogenously in the mothers and permanently present in the circulation. Naïve FVIII-KO females were treated with 2.10^{13} AAV8 vg/kg containing the FVIII-V3 transgene [23]. FVIII production peaked 2 weeks following treatment and gradually decreased over the next 10 weeks (**Fig. 3A and Fig. S5**). The decreased expression was not associated with the development of anti-FVIII neutralizing IgG (data not shown). At week 2, females were mated and became pregnant within 16 weeks. Endogenous FVIII was still detectable in pregnant mice at the time of transplacental delivery experiments (4.1±1.9 nM, range: 2.3 to 7.8 nM, **Fig. 3B**), concentrations that are in the range found in the plasma of human female HA carriers [29].

Three doses of KM33 FabFc were administered to AAV-treated FVIII-producing pregnant mice at E17.5. FVIII and FabFc were quantitated 4 hours later in the fetuses' plasma. While the transplacental delivery of KM33 FabFc was confirmed in the case of the two highest doses (i.e., 4 µg and 1.5 µg, **Fig. 3C**), that of FVIII was only marginal, and only detected with the highest FabFc dose (**Fig. 3D**). KM33 FabFc^{IHH} injection to FVIII-producing pregnant mice led to background transcytosis of FVIII to the fetuses. The data indicate that the constant endogenous production of FVIII by the mothers does not increase the amounts of FVIII that are transplacentally delivered to the fetuses by the FabFc.

Impact of the epitope specificity of the FabFc on the transplacental delivery of FVIII

In addition to KM33, that is specific for the C1 domain of FVIII, we generated BOIIB2 FabFc and BO2C11 FabFc, that are specific for the FVIII A2 and C2 domains, respectively (**Fig. S6A**). Both BOIIB2 and BO2C11 IgG originate from inhibitor-positive HA patients [21,22]. The three FabFc recognized FVIII in a dose-dependent manner (**Fig. 1B** and **Fig. S6B**) and inhibited FVIII pro-coagulant activity (**Table S1**). BO2C11 competed with VWF for binding to FVIII, while BOIIB2 did not (**Fig. S6C**). BOIIB2 and BO2C11 had equivalent affinities for FcRn (**Table S2**) and bound to FVIII *in vitro* at a large pH range (**Fig. S6D**). Naïve pregnant FVIII-KO mice were injected with FVIII pre-incubated with BOIIB2 or BO2C11 FabFc; levels of transcytosed FVIII were measured in the fetuses' plasma 4 hours later. While substantial levels of FVIII were detected in the fetuses' plasma in the case of BO2C11 FabFc, FVIII was poorly transplacentally delivered when injected with BOIIB2 FabFc (**Fig. 4A**). FVIII levels measured in fetuses' plasma were normalized as a function of the concentration of FabFc (**Fig. 4B**): the transplacental delivery of FVIII by KM33 FabFc was 5-fold greater than by BOIIB2 FabFc ($P<0.0001$) and 4-fold lower than by BO2C11 FabFc ($P=0.0001$), indicating that the epitope specificity of the FabFc impacts transcytosis efficacy.

Impact of the size of the complex on transplacental delivery

Using KM33 FabFc and BO2C11 FabFc, we investigated whether the size of the antigen impacts the transcytosis efficacy and, notably, whether full-length recombinant FVIII (that contains the B domain of the molecule, MW of 280 kDa) could be transplacentally delivered. FabFcs were incubated with full-length FVIII or with BDD-FVIII (MW of 165 kDa, used in all preceding experiments), prior to injection to pregnant mice. BO2C11 FabFc was also incubated with the FVIII C2 domain (MW of 19 kDa). For both FabFcs, transplacental delivery was greater for BDD-FVIII than full-length FVIII (**Fig. 4C**, $P<0.0001$). The transplacental delivery of C2 by BO2C11 FabFc was 100-fold greater than that of BDD-FVIII ($P=0.0002$). Because both KM33 and BO2C11 FabFc, in contrast to BOIIB2 FabFc, neutralize the binding of FVIII to VWF (**Fig. 1C** and **Fig. S6C**), we investigated whether BOIIB2 FabFc may foster the transplacental delivery of FVIII in the absence of endogenous VWF, the natural chaperone of FVIII in the blood. FVIII was however not better transcytosed by BOIIB2 FabFc in double FVIII/VWF-KO mice than in FVIII-KO mice (**Fig. 4D**).

Discussion

We investigated whether a therapeutic molecule may be intentionally delivered through the placenta during pregnancy from the blood of the mother to that of the fetus. We already documented in the mouse the transplacental delivery of the first domain of hemagglutinin [18], of pre-pro-insulin 1 [19] and of the two immunodominant FVIII A2 and C2 domains [18], all fused to the mouse Fcγ1. Other groups demonstrated the transfer from the mothers to the fetuses of Fc-fused erythropoietin [30] and beta-glucuronidase [16]. Our choice of human FVIII as a model antigen was motivated by the structural and biochemical complexity of this multi-domain glycoprotein, by the existence of different therapeutic variants of the molecule: full-

length, B domain-deleted and Fc-fused FVIII [31], by the availability of different patient-derived FVIII-specific monoclonal IgG and by its clinical relevance.

FVIII did not cross the placenta alone. This was true both when FVIII was injected as a bolus of 50 µg of exogenous FVIII (leading to a concentration of FVIII in the pregnant mice plasma of 15 to 108 nM 5 min following injection) or when FVIII was present as an endogenous molecule at a constant concentration of 2-8 nM in pregnant mice having undergone gene therapy. This is consistent with the documented absence of maternal FVIII in the cord blood of fetuses with severe HA, a phenomenon exploited in the past to diagnose HA before the birth of the babies [32].

The transplacental delivery of FVIII was explored in three experimental setups using pregnant mice: i) exogenous therapeutic FVIII was pre-incubated with engineered monovalent (FabFc) anti-FVIII IgG prior to injection to FVIII-deficient mice, ii) mice producing endogenous human FVIII following gene therapy were treated with an anti-FVIII FabFc, iii) FVIII-deficient mice were injected with a therapeutic Fc-fused FVIII (rFVIIIFc). In all cases, FVIII was delivered from the mothers' circulation to that of the fetuses. For FabFc-mediated FVIII transfer, the FabFc originated from neutralizing monoclonal anti-FVIII IgG, it was therefore not possible to measure the FVIII pro-coagulant activity in the fetuses' plasma. Yet, the amounts of FVIII protein reached up to 10% of the physiological FVIII plasma levels [26], i.e., levels that are sufficient to prevent minor bleeds in HA patients and provide protection against joint degradation [33]. This brings the theoretical proof-of-concept in favor of antenatal or pre-birth replacement therapy. In 4% of the cases, the birth of a baby with severe HA is complicated by intracranial hemorrhages that may be fatal or result in serious neurological impairment [34]. In this context, the supply of low amounts of pro-coagulant FVIII using non-inhibitory anti-FVIII FabFc to the fetal circulation at the time of delivery may protect the newborn from dramatic intracranial bleeds.

The preliminary results that motivated initiation of our study had shown transplacental delivery of the recombinant FVIII C2 domain by the native BO2C11 IgG, but not of BDD-FVIII (data not shown). Our decision to use engineered FabFc over native IgG was motivated by: i) previous observations of a superior transport of EPO-Fc fusion monomers over dimers through the respiratory eptithelium [30]; ii) reduced size of FabFc (100 kDa) as compared to that of IgG (150 kDa), iii) FabFc monovalency as opposed to IgG bivalency that warrants a lower size of the antibody/antigen complexes, a critical parameter in the case of FVIII where binding of 2 FVIII molecules to one IgG would lead to a >490 kDa complex, iv) reduced risk of forming large immune complexes on cell surfaces and crosslinking FcγR, v) potential for using cocktails of FabFc targeting different epitopes without crosslinking several antigens. All this should translate into improved FcRn-mediated transfer and reduced risk for triggering deleterious inflammatory responses.

The three different FVIII-specific FabFc used here yielded different amounts of transcytosed FVIII: FVIII was better transcytosed by BO2C11 than by KM33, and only poorly by BOIIB2 FabFc. The three FabFc share common features such as a human Fcγ1 fragment and a strong inhibitory activity towards FVIII (1400 to 7400 BU/mg). They however differ in terms of epitope specificity and capacity to prevent or not the binding of VWF to FVIII. VWF is the natural chaperone for FVIII in blood; the interaction between both molecules is indispensable to prevent the rapid FVIII elimination [35]. The interaction involves key residues in the C1 and C2 FVIII domains [36]. In our experiments, exogenous FVIII was injected in amounts that exceed the binding capacity of endogenous VWF; accordingly, FVIII was rapidly eliminated from the mothers' blood within the 4 hours. The fast elimination of FVIII from the mothers' circulation and its accumulation in the mothers' liver and spleen probably account at least in part for the poor transplacental delivery of FVIII, as a consequence of insufficient amounts of circulating FVIII for an insufficient amount of time. However, in mice treated with AAV-FVIII,

the endogenous production of FVIII at levels that do not saturate endogenous VWF failed to improve FabFc-mediated transplacental FVIII delivery. The A2 domain-specific BOIIB2 FabFc, that does not compete with VWF for binding to FVIII, failed to mediate FVIII transcytosis both in the presence and absence of endogenous VWF. Taken together, the latter observations suggest that VWF is not the main contributor to the limited transplacental FVIII delivery.

It is tempting to interpret the results of the increased FVIII delivery by the C1 or C2 domain-specific FabFc, in terms of promiscuity of the FVIII light chain. The FVIII light chain is implicated in FVIII binding to catabolic receptors such as LRP [37]. Interestingly, the mouse placenta expresses several receptors implicated in FVIII catabolism in the mouse [38] or by human cells [39,40]. We and others have shown that both C domains play a key role in FVIII endocytosis by human and murine dendritic cells [41,42]. The important residues targeted by the paratopes of KM33 and BO2C11 in the C1 and C2 domains have been identified: mutations to Ala of Arg2090, Lys2092, Phe2093 in C1 and of Arg2215 and Arg2020 in C2 abrogate the binding of the antibodies to FVIII [41,42]. Importantly, positively charged His, Lys and Arg residues favor binding to cell membranes. We hypothesize that the FVIII C1 and/or C2 domains engage unknown molecular interactions following FVIII internalization in the early endosomes of the syncytiotrophoblast. Such interactions may favor the routing of FVIII towards lysosomal degradation rather than towards recycling endosomes. BIVV001 is a recently described molecule with a largely extended half-life that is independent from binding to endogenous VWF [43]. In BIVV001, the C1 and C2 domains and part of the A3 domain are shielded by a recombinant D'D3 moiety [44]. Whether BIVV001 demonstrates increased transplacental delivery as compared to FVIII molecules that retain C1/C2-dependent binding promiscuity, shall be investigated as soon as the molecule is commercially available.

The size of the molecules appeared as a critical parameter in the potency for transplacental delivery. This result is potentially biased in the case of larger molecules, where the engagement of additional non-FcRn receptors in the early endosome of the syncytiotrophoblast may favor routing of the molecules towards the lysosomal degradation pathway. Indeed, full-length FVIII, which was less transcytosed than BDD-FVIII, contains a B domain that is rich in N-linked glycans and interacts with additional catabolic receptors [45]. Conversely, the C2 domain was extremely well transcytosed by BO2C11 FabFc, that binds and shields its charged amino-acids [42,46]. Likewise, the FVIII/KM33 FabFc complex was better transcytosed than Fc-fused FVIII, for which charged residues in the C1 domain remain accessible.

Our results provide the proof-of-concept that proteins can be transferred from mothers to fetuses using engineered monovalent IgG. Owing to differences in the structure of the placenta and timing of development of the fetal immune system between mice and human, our approach will be tested in alternative animal models in the future. In the mice, we identify the careful choice of the epitope targeted by the FabFc and the shielding of charged amino-acid residues to reduce protein promiscuity, as key parameters to ensure optimal transplacental delivery. We also demonstrate that protein transfer from the mother to the fetus may be achieved in different settings. Already existing therapeutic Fc-fused molecules (e.g., rFVIIIFc, rFIXFc, monoclonal antibodies, …) may be directly administered during pregnancy. Alternatively, FabFc may be injected alone when the protein is expressed endogenously in the mothers in sufficient amounts, or as a preformed complex with the exogenous recombinant protein. The transfer of proteins from mothers to fetuses may have clinical repercussions in the context of replacement therapy, for instance in the case of monogenic coagulation or lysosomal disorders [16], as well as to shape immune repertoires during immune system ontogeny, so as to favor the generation of protein-specific regulatory T cells and establishment of long-lasting active immune tolerance [18].

Authors contributions:

Designed the research	SLD, CD, OC, PL, VP
Performed the experiments	AM, MBJ, ARR, VD, SD, ML, AA, RN, IP, JDD
Analyzed the data	AM, MBJ, ARR, SD, SLD
Contributed essential material	JMI, AN
Wrote the article	AM, SLD

The authors declare no conflict of interest relevant to this work. JMI, AN are inventors on a patent licensed to BioMarin.

Acknowledgements

We thank Dr Pierre Bruhns (Institut Pasteur, France), Dr Sune Justesen (Immunitrack, Denmark) for providing us with mouse FcγR-expressing cells and mouse FcRn, respectively, and the staff from "Centre d'Expérimentation Fonctionnelle" at Centre de Recherche des Cordeliers (Paris) for assistance. Novoeight, Eloctate and Kovaltry were kind gifts from Novo Nordisk A/S (Måløv, Denmark), Sanofi-Genzyme (Cambridge, MA) and Swedish Orphan Biovitrum AB (Stockholm, Sweden), and Bayer Biopharmaceutical (Berkeley, Ca), respectively. Imaging was performed at the Centre d'Histologie, d'Imagerie Cellulaire et de Cytométrie (CHIC), a member of the Sorbonne Université Cell Imaging and Flow Cytometry network (LUMIC) and UPD cell imaging networks.

This work was supported by Institut National de la Santé et de la Recherche Médicale (INSERM), Centre National de la Recherche Scientifique (CNRS), Sorbonne Université, Université de Paris, Assistance Publique des Hôpitaux de Paris and funded by the European Union's Horizon 2020 research and innovation program under the Marie Sklodowska-Curie

grant agreement n°859974 (EDUC8) and by grants from Agence National de la Recherche (ANR-18-CE17-0010-02, n°18181LL, Exfiltrins), Sanofi-Genentech (Waltham, MA) and (Swedish Orphan Biovitrum AB (Höllviksnäs, Sweden), and CSL-Behring (Paris, France). AM, MBJ and ARR were recipients of fellowships from Agence National de la Recherche (ANR-18-CE17-0010-02, n° 18181LL) from Ministère de l'Enseignement supérieur, de la Recherche et de l'Innovation and from MSCA-ITN EDUC8 (n°859974).

References

1 Brosens I, Pijnenborg R, Vercruysse L, Romero R. The "great obstetrical syndromes" are associated with disorders of deep placentation. *Am J Obstet Gynecol* 2011; **204**: 193–201.

2 Nardi N, Brito-Zerón P, Ramos-Casals M, Aguiló S, Cervera R, Ingelmo M, Font J. Circulating auto-antibodies against nuclear and non-nuclear antigens in primary Sjögren's syndrome: prevalence and clinical significance in 335 patients. *Clin Rheumatol* 2006; **25**: 341–6.

3 Moise KJ. Fetal anemia due to non-Rhesus-D red-cell alloimmunization. *Semin Fetal Neonatal Med* 2008; **13**: 207–14.

4 Burrows RF, Kelton JG. Fetal thrombocytopenia and its relation to maternal thrombocytopenia. *N Engl J Med* 1993; **329**: 1463–6.

5 Ellinger I, Schwab M, Stefanescu A, Hunziker W, Fuchs R. IgG transport across trophoblast-derived BeWo cells: a model system to study IgG transport in the placenta. *Eur J Immunol* 1999; **29**: 733–44.

6 Antohe F, Rădulescu L, Gafencu A, Gheţie V, Simionescu M. Expression of functionally active FcRn and the differentiated bidirectional transport of IgG in human placental endothelial cells. *Hum Immunol* 2001; **62**: 93–105.

7 McCarthy KM, Yoong Y, Simister NE. Bidirectional transcytosis of IgG by the rat neonatal Fc receptor expressed in a rat kidney cell line: a system to study protein transport across epithelia. *J Cell Sci* 2000; **113 (Pt 7)**: 1277–85.

8 Ward ES, Martinez C, Vaccaro C, Zhou J, Tang Q, Ober RJ. From sorting endosomes to exocytosis: association of Rab4 and Rab11 GTPases with the Fc receptor, FcRn, during recycling. *Mol Biol Cell* 2005; **16**: 2028–38.

9 Kohler PF, Farr RS. Elevation of cord over maternal IgG immunoglobulin: evidence for an active placental IgG transport. *Nature* 1966; **210**: 1070–1.

10 Malek A, Sager R, Schneider H. Maternal-fetal transport of immunoglobulin G and its subclasses during the third trimester of human pregnancy. *Am J Reprod Immunol N Y N 1989* 1994; **32**: 8–14.

11 Halliday R. Prenatal and postnatal transmission of passive immunity to young rats. *Proc R Soc Lond B Biol Sci* 1955; **144**: 427–30.

12 Appleby P, Catty D. Transmission of immunoglobulin to foetal and neonatal mice. *J Reprod Immunol* 1983; **5**: 203–13.

13 Jones EA, Waldmann TA. The mechanism of intestinal uptake and transcellular transport of IgG in the neonatal rat. *J Clin Invest* 1972; **51**: 2916–27.

14 Cinicola B, Conti MG, Terrin G, Sgrulletti M, Elfeky R, Carsetti R, Fernandez Salinas A, Piano Mortari E, Brindisi G, De Curtis M, Zicari AM, Moschese V, Duse M. The Protective Role of Maternal Immunization in Early Life. *Front Pediatr* 2021; **9**.

15 Rottenstreich A, Zarbiv G, Oiknine-Djian E, Zigron R, Wolf DG, Porat S. Efficient Maternofetal Transplacental Transfer of Anti- Severe Acute Respiratory Syndrome Coronavirus 2 (SARS-CoV-2) Spike Antibodies After Antenatal SARS-CoV-2 BNT162b2 Messenger RNA Vaccination. *Clin Infect Dis Off Publ Infect Dis Soc Am* 2021; **73**: 1909–12.

16 Grubb JH, Vogler C, Tan Y, Shah GN, MacRae AF, Sly WS. Infused Fc-tagged beta-glucuronidase crosses the placenta and produces clearance of storage in utero in mucopolysaccharidosis VII mice. *Proc Natl Acad Sci U S A* 2008; **105**: 8375–80.

17 Rueff-Juy D, Faure M, Drapier A-M, Cazenave P-A. Role of Maternal Ig in the Induction of Cκ-Specific CD8+ T Cell Tolerance. *J Immunol* American Association of Immunologists; 1998; **161**: 721–8.

18 Gupta N, Culina S, Meslier Y, Dimitrov J, Arnoult C, Delignat S, Gangadharan B, Lecerf M, Justesen S, Gouilleux-Gruart V, Salomon BL, Scott DW, Kaveri SV, Mallone R, Lacroix-Desmazes S. Regulation of immune responses to protein therapeutics by transplacental induction of T cell tolerance. *Sci Transl Med* 2015; **7**: 275ra21.

19 Culina S, Gupta N, Boisgard R, Afonso G, Gagnerault M-C, Dimitrov J, Østerbye T, Justesen S, Luce S, Attias M, Kyewski B, Buus S, Wong FS, Lacroix-Desmazes S, Mallone R. Materno-Fetal Transfer of Preproinsulin Through the Neonatal Fc Receptor Prevents Autoimmune Diabetes. *Diabetes* 2015; **64**: 3532–42.

20 van den Brink EN, Turenhout EA, Bovenschen N, Heijnen BG, Mertens K, Peters M, Voorberg J. Multiple VH genes are used to assemble human antibodies directed toward the A3-C1 domains of factor VIII. *Blood* 2001; **97**: 966–72.

21 Jacquemin MG, Desqueper BG, Benhida A, Vander Elst L, Hoylaerts MF, Bakkus M, Thielemans K, Arnout J, Peerlinck K, Gilles JG, Vermylen J, Saint-Remy JM. Mechanism and kinetics of factor VIII inactivation: study with an IgG4 monoclonal antibody derived from a hemophilia A patient with inhibitor. *Blood* 1998; **92**: 496–506.

22 Jacquemin M, Gilles JG, Saint-Remy J-M. Antibodies binding to the A2 domain of FVIII and inhibiting coagulation activity. 2010.

23 McIntosh J, Lenting PJ, Rosales C, Lee D, Rabbanian S, Raj D, Patel N, Tuddenham EGD, Christophe OD, McVey JH, Waddington S, Nienhuis AW, Gray JT, Fagone P, Mingozzi F, Zhou S-Z, High KA, Cancio M, Ng CYC, Zhou J, et al. Therapeutic levels of FVIII following a single peripheral vein administration of rAAV vector encoding a novel human factor VIII variant. *Blood* 2013; **121**: 3335–44.

24 Dimitrov JD, Roumenina LT, Plantier J-L, Andre S, Saboulard D, Meslier Y, Planchais C, Jacquemin M, Saint-Remy J-M, Atanasov BP, Kaveri SV, Lacroix-Desmazes S. A human FVIII inhibitor modulates FVIII surface electrostatics at a VWF-binding site distant from its epitope. *J Thromb Haemost JTH* 2010; **8**: 1524–31.

25 Jacquemin M, Benhida A, Peerlinck K, Desqueper B, Vander Elst L, Lavend'homme R, d'Oiron R, Schwaab R, Bakkus M, Thielemans K, Gilles JG, Vermylen J, Saint-Remy JM. A human antibody directed to the factor VIII C1 domain inhibits factor VIII cofactor activity and binding to von Willebrand factor. *Blood* 2000; **95**: 156–63.

26 Butenas S, Parhami-Seren B, Undas A, Fass DN, Mann KG. The "normal" factor VIII concentration in plasma. *Thromb Res* 2010; **126**: 119–23.

27 Navarrete A, Dasgupta S, Delignat S, Caligiuri G, Christophe OD, Bayry J, Nicoletti A, Kaveri SV, Lacroix-Desmazes S. Splenic marginal zone antigen-presenting cells are critical for the primary allo-immune response to therapeutic factor VIII in hemophilia A. *J Thromb Haemost JTH* 2009; **7**: 1816–23.

28 NC3RS.org.

29 Leebeek FWG, Duvekot J, Kruip MJHA. How I manage pregnancy in carriers of hemophilia and patients with von Willebrand disease. *Blood* 2020; **136**: 2143–50.

30 Bitonti AJ, Dumont JA, Low SC, Peters RT, Kropp KE, Palombella VJ, Stattel JM, Lu Y, Tan CA, Song JJ, Garcia AM, Simister NE, Spiekermann GM, Lencer WI, Blumberg RS. Pulmonary delivery of an erythropoietin Fc fusion protein in non-human primates through an immunoglobulin transport pathway. *Proc Natl Acad Sci U S A* 2004; **101**: 9763–8.

31 Lieuw K. Many factor VIII products available in the treatment of hemophilia A: an embarrassment of riches? *J Blood Med* 2017; **8**: 67–73.

32 Saxena R, Ranjan R. Prenatal Diagnosis of Hemophilia A and B. *J Mol Biol Mol Imaging* 2014; **Volume 1**: 7.

33 den Uijl IEM, Fischer K, Van Der Bom JG, Grobbee DE, Rosendaal FR, Plug I. Analysis of low frequency bleeding data: the association of joint bleeds according to baseline FVIII activity levels. *Haemoph Off J World Fed Hemoph* 2011; **17**: 41–4.

34 Singleton TC, Keane M. Diagnostic and therapeutic challenges of intracranial hemorrhage in neonates with congenital hemophilia: a case report and review. *Ochsner J* 2012; **12**: 249–53.

35 Lenting PJ, VAN Schooten CJM, Denis CV. Clearance mechanisms of von Willebrand factor and factor VIII. *J Thromb Haemost JTH* 2007; **5**: 1353–60.

36 Chiu P-L, Bou-Assaf GM, Chhabra ES, Chambers MG, Peters RT, Kulman JD, Walz T. Mapping the interaction between factor VIII and von Willebrand factor by electron microscopy and mass spectrometry. *Blood* 2015; **126**: 935–8.

37 Lenting PJ, Neels JG, van den Berg BM, Clijsters PP, Meijerman DW, Pannekoek H, van Mourik JA, Mertens K, van Zonneveld AJ. The light chain of factor VIII comprises a binding site for low density lipoprotein receptor-related protein. *J Biol Chem* 1999; **274**: 23734–9.

38 Wassef L, Shete V, Hong A, Spiegler E, Quadro L. β-Carotene supplementation decreases placental transcription of LDL receptor-related protein 1 in wild-type mice and stimulates placental β-carotene uptake in marginally vitamin A-deficient mice. *J Nutr* 2012; **142**: 1456–62.

39 Cao C, Pressman EK, Cooper EM, Guillet R, Westerman M, O'Brien KO. Placental heme receptor LRP1 correlates with the heme exporter FLVCR1 and neonatal iron status. *Reprod Camb Engl* 2014; **148**: 295–302.

40 Ali SR, Fong JJ, Carlin AF, Busch TD, Linden R, Angata T, Areschoug T, Parast M, Varki N, Murray J, Nizet V, Varki A. Siglec-5 and Siglec-14 are polymorphic paired receptors that modulate neutrophil and amnion signaling responses to group B Streptococcus. *J Exp Med* 2014; **211**: 1231–42.

41 Wroblewska A, van Haren SD, Herczenik E, Kaijen P, Ruminska A, Jin S-Y, Zheng XL, van den Biggelaar M, ten Brinke A, Meijer AB, Voorberg J. Modification of an exposed loop in the C1 domain reduces immune responses to factor VIII in hemophilia A mice. *Blood* 2012; **119**: 5294–300.

42 Gangadharan B, Ing M, Delignat S, Peyron I, Teyssandier M, Kaveri SV, Lacroix-Desmazes S. The C1 and C2 domains of blood coagulation factor VIII mediate its endocytosis by dendritic cells. *Haematologica* 2017; **102**: 271–81.

43 Seth Chhabra E, Liu T, Kulman J, Patarroyo-White S, Yang B, Lu Q, Drager D, Moore N, Liu J, Holthaus AM, Sommer JM, Ismail A, Rabinovich D, Liu Z, van der Flier A, Goodman A, Furcht C, Tie M, Carlage T, Mauldin R, et al. BIVV001, a new class of factor VIII replacement for hemophilia A that is independent of von Willebrand factor in primates and mice. *Blood* 2020; **135**: 1484–96.

44 Fuller JR, Knockenhauer KE, Leksa NC, Peters RT, Batchelor JD. Molecular determinants of the factor VIII/von Willebrand factor complex revealed by BIVV001 cryo-electron microscopy. *Blood* 2021; **137**: 2970–80.

45 Bovenschen N, Rijken DC, Havekes LM, van Vlijmen BJM, Mertens K. The B domain of coagulation factor VIII interacts with the asialoglycoprotein receptor. *J Thromb Haemost JTH* 2005; **3**: 1257–65.

46 Spiegel PC, Jacquemin M, Saint-Remy J-MR, Stoddard BL, Pratt KP. Structure of a factor VIII C2 domain–immunoglobulin G4κ Fab complex: identification of an inhibitory antibody epitope on the surface of factor VIII. *Blood* 2001; **98**: 13–9.

Tables

Table 1. Kinetic parameters that govern the binding of FabFc to the mouse FcRn

Binding to mFcRn	k_{on} ($M^{-1}.s^{-1}$)	k_{off} (s^{-1})	K_D (nM)	Chi^2
KM33 FabFc	4.5×10^{5}	4.32×10^{-4}	0.96	1.55
KM33 FabFc^{IHH}	ND	ND	ND	-
KM33 FabFc^{N297A}	4.59×10^{5}	3.83×10^{-4}	1.2	3.75

The binding kinetics of the different FabFc variants were studied by surface plasmon resonance at pH 6 with association times of 4 min and dissociation times of 5 min for FabFc concentration ranging from 0.04 to 25 nM. Biotinylated mouse FcRn was immobilized on streptavidin-coated chips at 500 RU. ND: no detectable signal.

Legends to figures

Figure 1. Transplacental delivery of exogenous FVIII is mediated by KM33 FabFc

Panel A. The KM33 FabFc includes variable heavy (VH) and light (VL) chains of the human anti-FVIII IgG KM33 and the constant regions of the human IgG1 and of the kappa light chain. The Fc fragment is stabilized by addition of a linker. Panel B. Binding of FVIII to KM33 FabFc. Human full-length FVIII (Advate®) was incubated in serial dilutions on plates coated with KM33 FabFc and IgG. The graph depicts the binding of FVIII detected using a secondary biotinylated anti-human FVIII IgG. Binding is expressed as arbitrary units (AU) as mean±standard deviation (SD) based on the optical density measured at 492 nm, in two independent experiments. Panel C. Inhibition of the binding of FVIII to VWF by KM33 FabFc. KM33 FabFc and IgG were incubated with full-length FVIII (0.2 nM, Advate ®), prior to incubation on VWF (10 µg/ml, Wilfactin ®)-coated ELISA plates. FVIII binding was detected using a mouse anti-A2 domain IgG and is expressed as the percentage of inhibition of the binding of FVIII incubated alone (n=3, mean±SD). Panel D. KM33 FabFc-mediated FVIII transplacental delivery. Naïve pregnant FVIII-KO mice (n=3-5) at E17.5 of gestation were injected intravenously with FVIII alone (50 µg) or FVIII pre-incubated with KM33 FabFc, KM33 FabFc^{N297A} or KM33 FabFc^{IHH} (30 µg). Blood was collected from the fetuses 4 hours after injection of the mothers. FVIII (left panel), the FVIII/KM33 FabFc complex (middle panel) and KM33 FabFc (right panel) were then quantified in the fetuses' plasma using three different ELISA setups. The graphs depict the molar concentrations of the different molecules. Each individual dot represents a pool of 2 to 3 fetuses' plasma. The horizontal dotted line represents the threshold of FVIII, complex or FabFc detection (0.003, 0.003 and 0.005 nM, respectively). Differences were statistically assessed using the two-tailed non-parametric Mann-Whitney test. Horizontal lines depict the means.

Figure 2. *In vivo* stability of the FVIII/FabFc complex

KM33 FabFc alone (29.1 µg), rFVIIIFc alone (50 µg) or FVIII alone (50 µg) or pre-incubated with KM33 FabFc (29.1 µg) were injected intravenously to naïve E17.5 pregnant FVIII-KO mice (n=3-6). **Panels A and C.** Levels FVIII and KM33 FabFc in the mothers' and fetuses' circulation. Blood was collected from the pregnant mice (5 min and 4 hours after injection of the molecules) and from their fetuses (4 hours after). The graphs depict the concentration of FVIII and KM33 FabFc quantitated independently by ELISA, as already described (mean±SD). **Panels B and D.** Detection of FVIII in different organs. Mice were injected with FVIII (50 µg) alone or pre-incubated with equimolar amounts (29.1 µg) of KM33 FabFc or KM33 FabFc^{IHH}. Livers and spleens were collected 30 min later (Panel B) and placentas were collected 4 hours later (Panel D). Immunofluorescence on tissue sections was performed to detect FVIII, FabFc and/or syncytiotrophoblasts using a polyclonal sheep anti-human FVIII IgG (red, left panels on B and D), a goat anti-human Ig Fab (green, middle panels on B) and a rat anti-mouse Ly-6A/E antibody (green, middle panels on D), respectively. Nuclei were stained using Hoechst (blue). Images were acquired using a confocal microscope (63X) Zeiss LSM 710 and merged (right panels). The percentages of co-localization between FVIII and KM33 FabFc (panel B), or between FVIII and Ly6E (panel D and **Fig. S3**) are depicted on the right of each panel (n=10, mean±SD). **Panel E.** pH sensitivity of the interaction between FVIII and KM33 FabFc. KM33 FabFc (13 nM) was diluted in buffers with pH ranging from 3 to 8, prior to incubation on FVIII (2.5 µg/ml, Advate®)-coated ELISA plates. The residual binding is depicted in arbitrary units (optical density measured at 492 nm) (mean±SD of 2 independent experiments). **Panel F.** Transplacental delivery of rFVIIIFc. The amounts of rFVIIIFc were measured by ELISA in the fetuses' plasma 4 hours following injection to E17.5 pregnant mice, as explained. Each dot represents plasma pool from 2-3 fetuses. The red dots represent the amount of FVIII

transplacentally delivered by KM33 FabFc and are from Fig. 1D. Differences were statistically assessed using the two-tailed non-parametric Mann-Whitney test. Horizontal lines depict the means (ns: non-significant).

Figure 3. Transplacental delivery of endogenous FVIII

Panel A. Kinetics of FVIII expression following gene therapy. Six-week old female FVIII-KO mice were administered intravenously with $2x10^{13}$ vg/kg of rAAV-HLP-codop-hFVIII-V3. FVIII antigen in plasma was measured by ELISA and is expressed in nM (horizontal bars depict means). Each dot represents one single mouse. **Panel B.** Endogenous FVIII levels in pregnant mice at the time of transplacental delivery experiments. FVIII-producing pregnant mice were injected with KM33 FabFc (0.15, 1.5 µg or 4 µg in 200 µL) or KM33 $FabFc^{IHH}$ (4 µg in 200 µL) at E17.5 (i.e., 4-18 weeks after gene therapy). FVIII was measured by ELISA in mothers' plasma 5 min later. **Panels C and D.** FVIII and FabFc transplacental delivery. The levels of transplacentally delivered KM33 FabFc (panel C) and FVIII (panel D) were measured in fetuses' plasma 4 hours following FabFc injection to pregnant mice. Each single dot is representative of a plasma pooled from 2 or 3 fetuses. The horizontal dotted lines represent the threshold of FVIII or FabFc detection (0.003 and 0.005 nM, respectively). Differences were statistically assessed using a two-tailed non-parametric Mann-Whitney test. Horizontal lines depict the means.

Figure 4. Effect of antigen size and epitope specificity of FabFc on transplacental delivery efficiency

Panels A and B. Transplacental delivery of exogenous FVIII by FabFc with different epitope specificities. FVIII was pre-incubated with the A2 domain-specific BOIIB2 FabFc or C2 domain-specific BO2C11 FabFc prior to injection to naïve E17.5 pregnant FVIII-KO mice

(n=3-4). Blood was collected from the fetuses 4 hours after injection of the mothers. FVIII (panel A) and FabFc (not shown) were quantified in the fetuses' plasma by ELISA. Panel A depicts the FVIII concentration with each individual dot representing a pool of 2 or 3 fetuses' plasma. The horizontal dotted line represents the threshold of FVIII detection. Panel B depicts the FVIII/FabFc molar ratio at 4 hours in the fetuses' plasma. Data shown for KM33 FabFc in panel A and B are from Fig. 1D and Fig. 2B, respectively. Panel C. Impact of the size on the transplacental delivery. KM33 FabFc and BO2C11 FabFc (25 µg or 29.1 µg) were incubated at equimolar concentrations with full-length FVIII (70µg) (FL, Helixate®) or with BDD-FVIII (50 µg, 150 nM) (BDD). BO2C11 FabFc (29 µg, 145 nM) was also incubated at equimolar concentrations with the recombinant FVIII C2 domain (5.5 µg, 145 nM). The molecular complexes were then injected to E17.5 pregnant FVIII-KO mice. FVIII or C2 concentrations were measured in the fetuses' plasma 4 hours later using dedicated ELISAs and are depicted on the graph. Each dot represents a pool of 2 to 3 fetuses' plasma. Data for transplacental delivery of BDD-FVIII by KM33 and BO2C11 FabFc are from Fig. 1D and panel A. Panel D. Effect of VWF on the transplacental delivery of FVIII. FVIII was pre-incubated with BOIIB2 FabFc prior to injection to E17.5 pregnant FVIII-KO or double FVIII/VWF-KO mice (n=2-4). FVIII concentration was detected in the fetuses' plasma 4 hours later with each dot representing the plasma pool from 2-3 fetuses. Data for transplacental delivery of FVIII by BOIIB2 FabFc in FVIII-KO mice are from panel A. Statistical differences were determined using the two-tailed non-parametric Mann-Whitney test (ns: non-significant). Horizontal lines depict the means.

Supplementary material

Supplementary methods

Binding of FabFc to the mouse FcRn. The binding kinetics of FabFc for FcRn were measured by surface plasmon resonance (Biacore, Cytiva). Biotinylated mouse FcRn (5 µg/mL, Immunitrack, København, Denmark) was immobilized on a streptavidin sensor chip (Cytiva, protein surface density of 0.5 ng/mm^2 or 500 resonance units (RU)). FabFc (0.04 to 25 nM) diluted in 100 mM Tris, 100 mM NaCl, 5% glycerol, and 0.1% tween 20 pH6, were injected at 30 µL/min at 25°C. Association and spontaneous dissociation phases were followed for 4 and 5 min, respectively. Chip surface was regenerated using 100 mM Tris, 100 mM NaCl pH7, at 30 µL/min for 30 seconds. Data were analysed using BIAevaluation version 4.1 software (Biacore Life Science). K_{on} and k_{off} were calculated using the Langmuir binding model, the constant affinity K_D was calculated as k_{off}/k_{on}.

Binding of FabFc to mouse FcγR. CHO-transfected cells with FLAG-tagged murine FcγRI (CD64) and FcγRIIb (CD32B) were a gift from Dr. Bruhns (Institut Pasteur, Paris, France) [1]. Cells were incubated with 10 nM of FabFcs in RPMI 1640, 0.5% FCS for 1 hour at 4°C followed by an incubation with a PE-conjugated goat F(ab')$_2$ anti-human Fc (Thermo Fisher Scientific, Waltham, Massachusetts). Binding of FabFc to mFcγRI or mFcγRIIb-expressing CHO cells was measured by flow cytometry (LSR II) following exclusion of dead cells with the fixable viability dye eFluor 780 (Thermo Fisher Scientific), and analysed using the FlowJo software (BD Biosciences, San Jose, CA, USA).

Inhibition of the functional activity of FVIII. The neutralizing activity of anti-FVIII FabFc and IgG was measured in a modified Bethesda assay [2,3]. Serial dilutions of FabFc and IgG starting from 16.7 nM were incubated in standard human plasma as a source of FVIII (Siemens Healthcare, Erlangen, Germany) for 2 hours at 37°C. The residual FVIII levels were measured in a FVIII chromogenic kit (Siemens Healthcare). Briefly, samples were incubated with activated coagulation factor IX and factor X for 3 minutes, followed by the addition of a chromogenic substrate for

activated factor X for 20 minutes. The optical density was measured at 405 nm. The inhibitory activity is expressed in Bethesda units (BU) per µg of protein, which corresponds to the inverse of the protein amount that yields to 50% FVIII inhibition.

Immuno-fluorescence on mouse tissues. To collect spleens and livers, mice were sacrificed 30 minutes following injection with FVIII with or without FabFc and perfused with pre-warm PBS (Life Technologies). To collect placentas, mice were sacrificed 4 hours after treatment. Organs were collected, stored in formaldehyde 4% (Sigma Aldrich) for 12 hours and incubated successively in solutions of 15% and 30% sucrose (Sigma Aldrich, St Louis, Missouri) for 12 hours each. Organs were frozen in liquid nitrogen and stored at -80°C until use. Eight µm sections were cut from frozen tissues with a LEICA CM1850 cryostat (Leica Biosystem, Wetzlar, Germany) and stuck onto Menzel Glaser superfrost slides (Thermo Scientific). For spleens and livers, tissues were fixed with 10% neutral buffered formalin (Sigma Aldrich) for 5 minutes at room temperature and permeabilized with 0.2% tween 20 (Sigma Aldrich) for 15 minutes at room temperature. Endogenous biotin and avidin were blocked (Invitrogen Waltham, Massachusetts). For placentas, tissues were fixed and permeabilized with cold acetone for 10 minutes. Fixed placentas were then blocked with PBS, 5% fetal calf serum, 1% BSA. KM33 FabFc was revealed with a biotinylated cross-absorbed goat anti-human Fab mouse (2043-08, Southern Biotech) and streptavidin conjugated to AF555 (S32355, Invitrogen). FVIII was revealed with the polyclonal sheep anti-human FVIII (SAF8C AP) and a mouse- and human-crossed absorbed donkey anti-sheep IgG conjugated to AF647 (A21448, Invitrogen). Syncytiotrophoblast cells were detected with a rat anti mouse Ly-6A/E or Sca-1 (14-5981-82, eBioscience™, Thermo Scientific) and a goat anti-rat IgG (H+L) conjugated to AF488 (A11006, Invitrogen). Microscope slides were mounted with Prolong gold antifade media (Invitrogen). Stained sections were visualized with a Zeiss LSM 710 confocal microscope (63X) (Zeiss, Iena, Germany), pictures were analyzed with Zeiss Zen software.

References

1 Mancardi DA, Iannascoli B, Hoos S, England P, Daëron M, Bruhns P. FcγRIV is a mouse IgE receptor that resembles macrophage FcεRI in humans and promotes IgE-induced lung inflammation. *J Clin Invest* American Society for Clinical Investigation; 2008; **118**: 3738–50.

2 Kasper CK, Aledort L, Aronson D, Counts R, Edson JR, van Eys J, Fratantoni J, Green D, Hampton J, Hilgartner M, Levine P, Lazerson J, McMillan C, Penner J, Shapiro S, Shulman NR. Proceedings: A more uniform measurement of factor VIII inhibitors. *Thromb Diath Haemorrh* 1975; **34**: 612.

3 Verbruggen B, Novakova I, Wessels H, Boezeman J, van den Berg M, Mauser-Bunschoten E. The Nijmegen modification of the Bethesda assay for factor VIII:C inhibitors: improved specificity and reliability. *Thromb Haemost* 1995; **73**: 247–51.

4 Chen H, Maul-Pavicic A, Holzer M, Huber M, Salzer U, Chevalier N, Voll RE, Hengel H, Kolb P. Detection and functional resolution of soluble immune complexes by an FcγR reporter cell panel. *EMBO Mol Med* 2022; **14**: e14182.

Supplementary Tables

Table S1. Inhibitory activity of the anti-FVIII IgG and FabFc towards pro-coagulant FVIII

	BU/µg	
	IgG1	**FabFc**
BOIIB2	6.1 ± 0.7	7.4 ± 2.7
KM33	0.9 ± 0.3	1.4 ± 0.4
BO2C11	7.1 ± 1.0	2.8 ± 0.4

The FVIII neutralizing activity of the parent human IgG and corresponding engineered FabFc were measured in an in vitro functional pro-coagulant Bethesda assay. BU: Bethesda units.

Table S2. Kinetic parameters that govern the binding of FabFc to the mouse FcRn

Binding to mFcRn	k_{on} ($M^{-1}.s^{-1}$)	k_{off} (s^{-1})	K_D (nM)	Chi^2
BO2C11 FabFc	1.8×10^{5}	2.8×10^{-4}	1.5	2.8
BOIIB2 FabFc	1.7×10^{5}	4.7×10^{-4}	2.7	3.3

The binding kinetics of the different FabFc variants were studied by surface plasmon resonance at pH 6 with association times of 4 min and dissociation times of 5 min for FabFc concentration ranging from 0.04 to 25 nM. Biotinylated mouse FcRn was immobilized on streptavidin-coated chips at 500 RU. ND: no detectable signal.

Supplementary figures

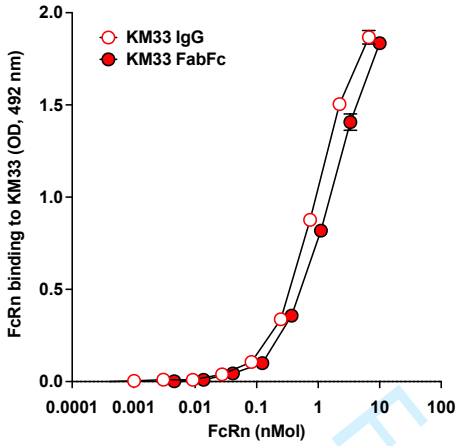

Figure S1. Binding of recombinant mouse FcRn to KM33 IgG and FabFc. KM33 IgG (150 kDa) and FabFc (100 kDa) were immobilized at 1 µg/ml on ELISA plates. Plates were blocked with PBS, 3% BSA, 0.1% tween 20. Biotinylated mouse FcRn was incubated in serial dilutions in blocking buffer. After washing, the bound FcRn was revealed using streptavidin-peroxidase and the peroxidase substrate. The graph depicts the intensity of binding of mouse FcRn expressed in arbitrary units (OD: Optical density measured at 492 nm).

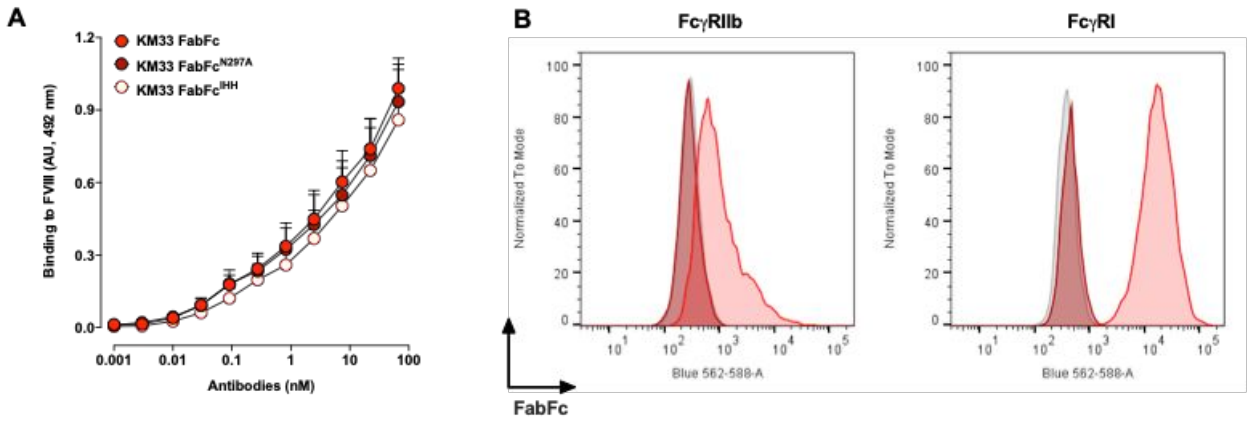

Figure S2. Validation of KM33 FabFc, KM33 FabFc^{N297A}, and KM33 FabFc^{IHH}. Panel A. Binding of KM33 FabFc, KM33 FabFc^{N297A} and KM33 FabFc^{IHH} to FVIII. The different FabFc were incubated in serial dilutions on plates coated with human full-length FVIII (Advate®). The graph depicts the binding of the FabFc detected using a secondary anti-human Fc IgG, expressed in arbitrary units (AU) as mean ± SD, based on the optical density measured at 492 nm in three independent experiments. Panel B. Binding of KM33 FabFc and KM33 FabFc^{N297A} to murine FcγRs. The FabFc (10 nM) were incubated with CHO cells expressing the mouse FcγRI (CD64) or FcγRIIb (CD32b). Bound FabFcs were detected with a goat anti-human IgG F(ab')$_2$ conjugated to PE. The fluorescence was measured by flow cytometry (BD LSR 2). The histograms show the binding of KM33 FabFc in red, KM33 FabFc^{N297A} in dark red and cells incubated alone in grey. Data are representative of 3 independent experiments. Of note, KM33 FabFc also bound to human FcγR expressed by transduced cells [4], but did not trigger signaling (data not shown).

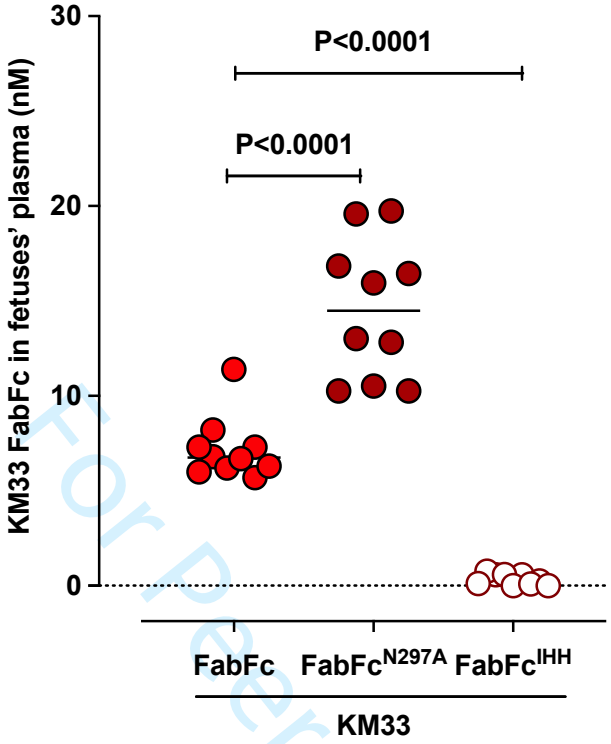

Figure S3. Transplacental delivery of KM33 FabFc. Naïve pregnant FVIII-KO mice (n=3-4) at E17.5 of gestation were injected intravenously with FVIII (50 µg) pre-incubated with KM33 FabFc, KM33 FabFc^{N297A} or KM33 FabFc^{IHH} (29.1 µg). Blood was collected from the fetuses 4 hours after injection of the mothers. The different KM33 FabFc variants were then quantified in the fetuses' plasma by ELISA. The graphs depict the molar concentrations of the different FabFc. Each individual dot represents a pool of 2 to 3 fetuses' plasma. The horizontal dotted line represents the threshold of FabFc detection (0.005 nM). Differences were statistically assessed using the two-tailed non-parametric Mann-Whitney test. Horizontal lines depict the means.

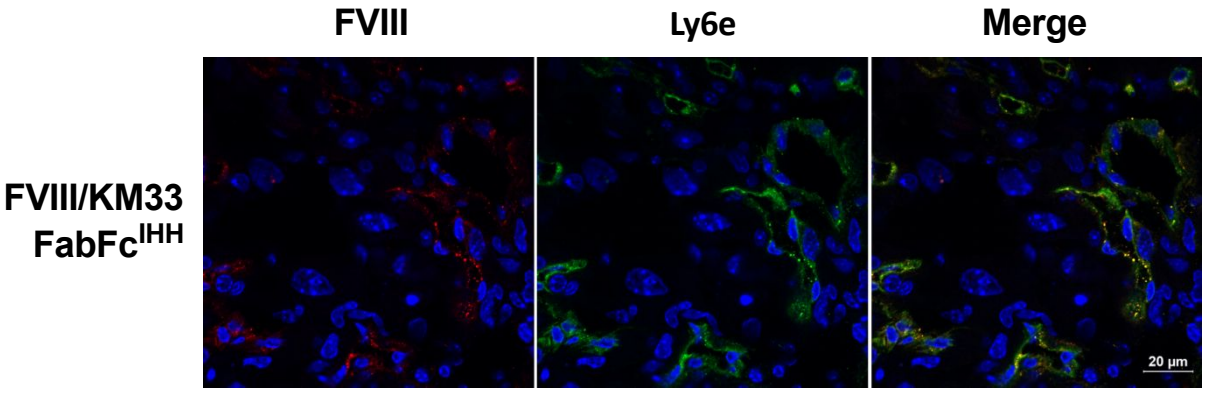

Fig S4. Accumulation of FVIII in the placenta. Mice were injected with FVIII (50 µg) pre-incubated with equimolar amounts (29.1 µg) of KM33 FabFc^{IHH}. Placentas were collected 4 hours later. Immunofluorescence on placenta sections was performed to detect FVIII or syncytiotrophoblasts using a polyclonal sheep anti-human FVIII IgG (red, left panel), and a rat anti-Ly-6A/E antibody (green, middle panel). Nuclei were stained using Hoechst (blue). Images were acquired using a confocal microscope (63X) Zeiss LSM 710 and merged (right panels).

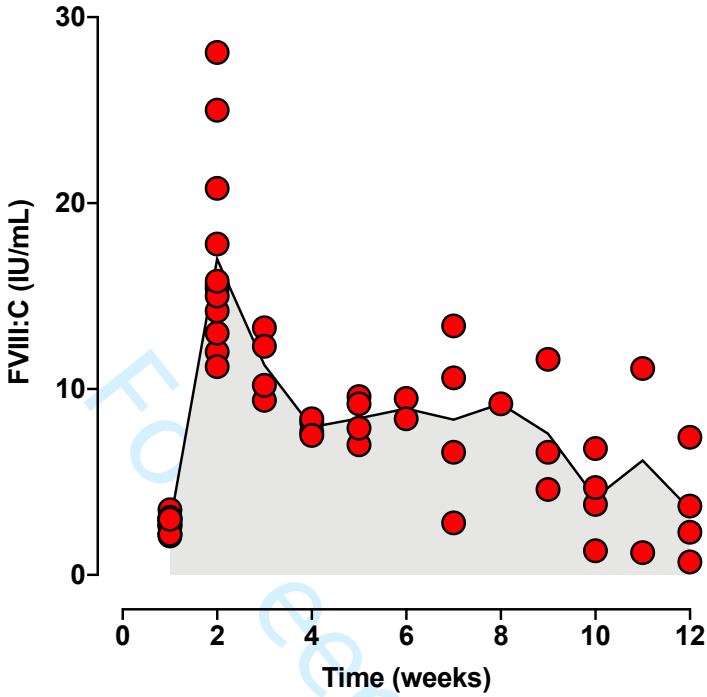

Figure S5. Kinetics of FVIII expression following gene therapy. Six-week old female FVIII-KO mice were administered intravenously with $2x10^{13}$ vg/kg of rAAV-HLP-codop-hFVIII-V3. FVIII activity (FVIII:C) in plasma was measured using a chromogenic assay and is expressed in IU/ml. Each dot represents one single mouse. The curve connecting mean values is shown as a plain line.

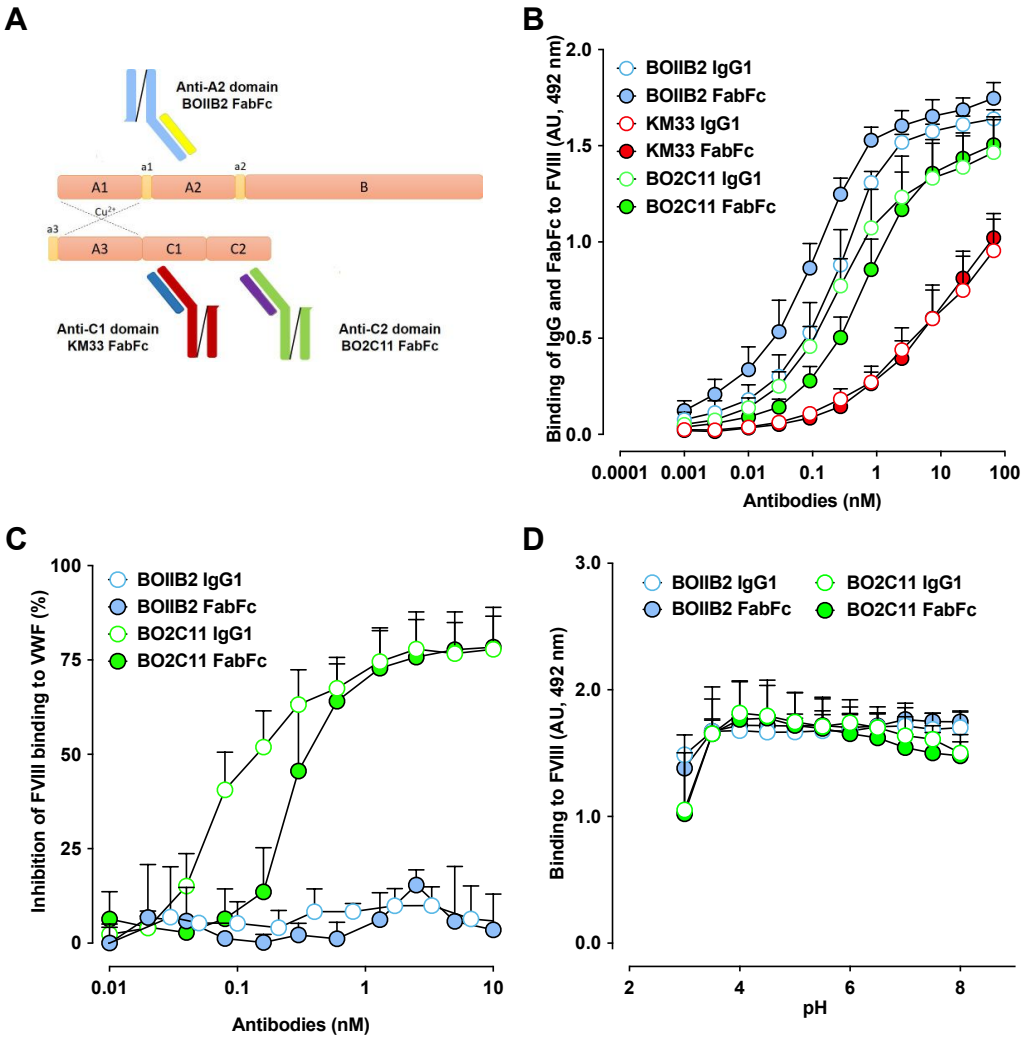

Figure S6. Validation of anti-FVIII FabFc. Panel A. Structure and specificity of FabFc. The 3 FabFc includes variable heavy (VH) and light (VL) chains of the A2-specific BOIIB2, C1-specific KM33 or C2-specific BO2C11 human anti-FVIII IgG1, as well as the constant regions from the human IgG1 and from the human kappa light chain. The Fc fragments are stabilized by addition of a linker. The panel also depicts the heterodimeric structure of human pro-coagulant FVIII with the heavy chain (A1-A2-B domains) and light chain (A3-C1-C2 domains). Panel B. Binding of BOIIB2, KM33 and BO2C11 FabFc to FVIII. FabFc and IgG were incubated in serial dilutions on FVIII (Advate®)-coated plates. The graph depicts the binding of the FabFc and IgG detected using a secondary anti-human Fc IgG. Binding is expressed as arbitrary units (AU) as mean±SD based on the optical density measured at 492 nm, in three independent experiments. Panel C. Inhibition of the binding of FVIII to VWF by BOIIB2 and BO2C11 FabFc. FabFc and IgG were incubated with full-length FVIII (0.2 nM, Advate ®), prior to incubation on VWF (10 µg/ml, Wilfactin ®)-coated ELISA plates. FVIII binding was detected using a mouse anti-A2 domain IgG and is expressed as the percentage of inhibition of the binding of FVIII incubated alone (n=3, mean±SD). Panel D. pH sensitivity of the interaction between FVIII and BOIIB2 and BO2C11 FabFc. FabFc (13 nM) were diluted in buffers with pH ranging from 3 to 8, prior to incubation on FVIII (2.5 µg/ml, Advate®)-coated ELISA plates. The residual binding is depicted in arbitrary units (optical density measured at 492 nm) (mean±SD of 2 independent experiments).

Figure 1

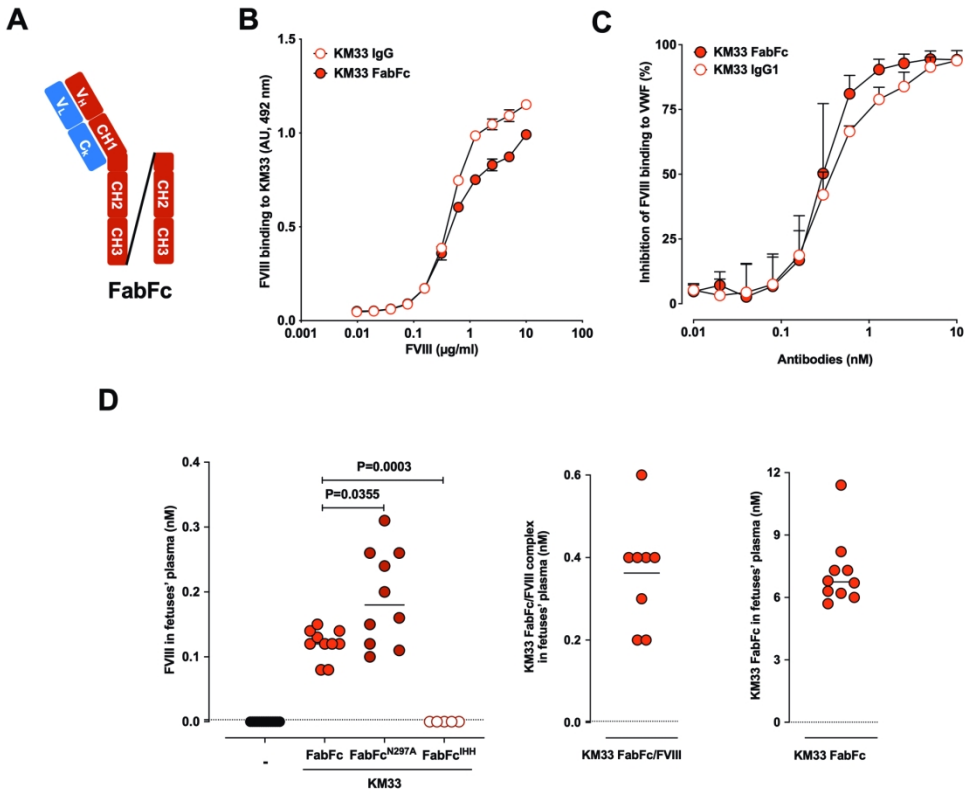

Figure 1

173x158mm (300 x 300 DPI)

Figure 2

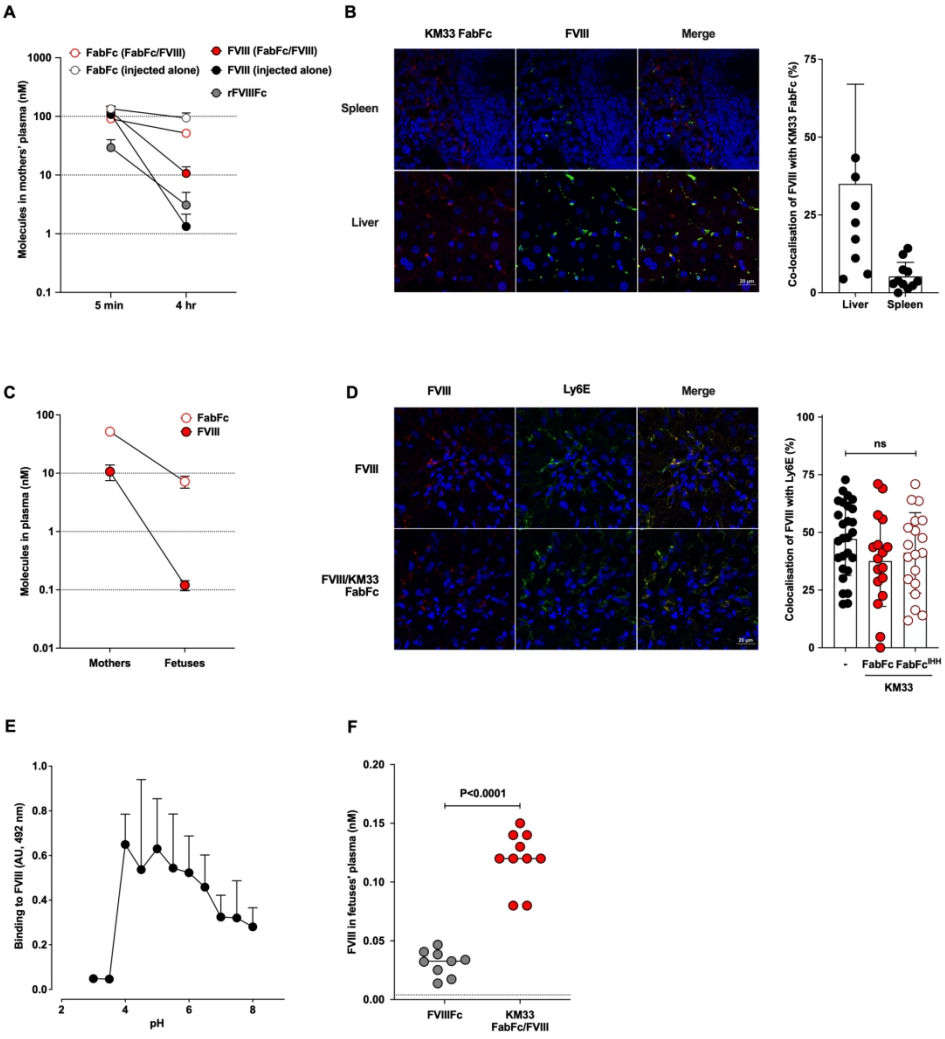

Figure 2

173x194mm (300 x 300 DPI)

Figure 3

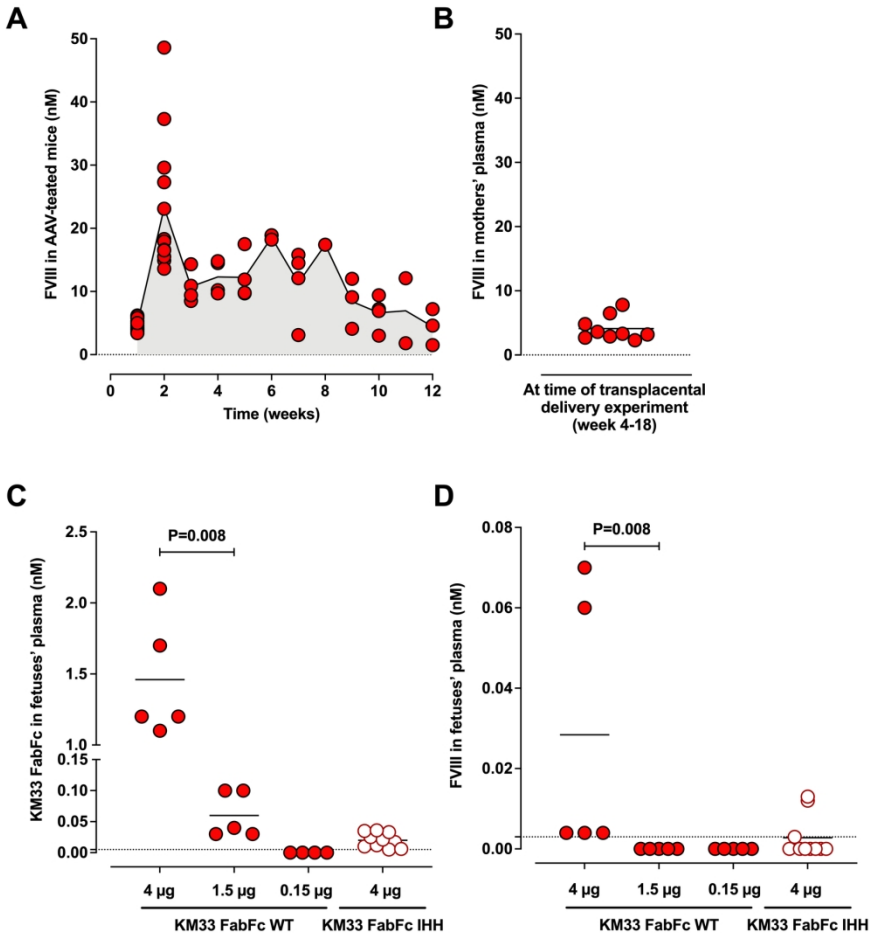

Figure 3

173x178mm (300 x 300 DPI)

Figure 4

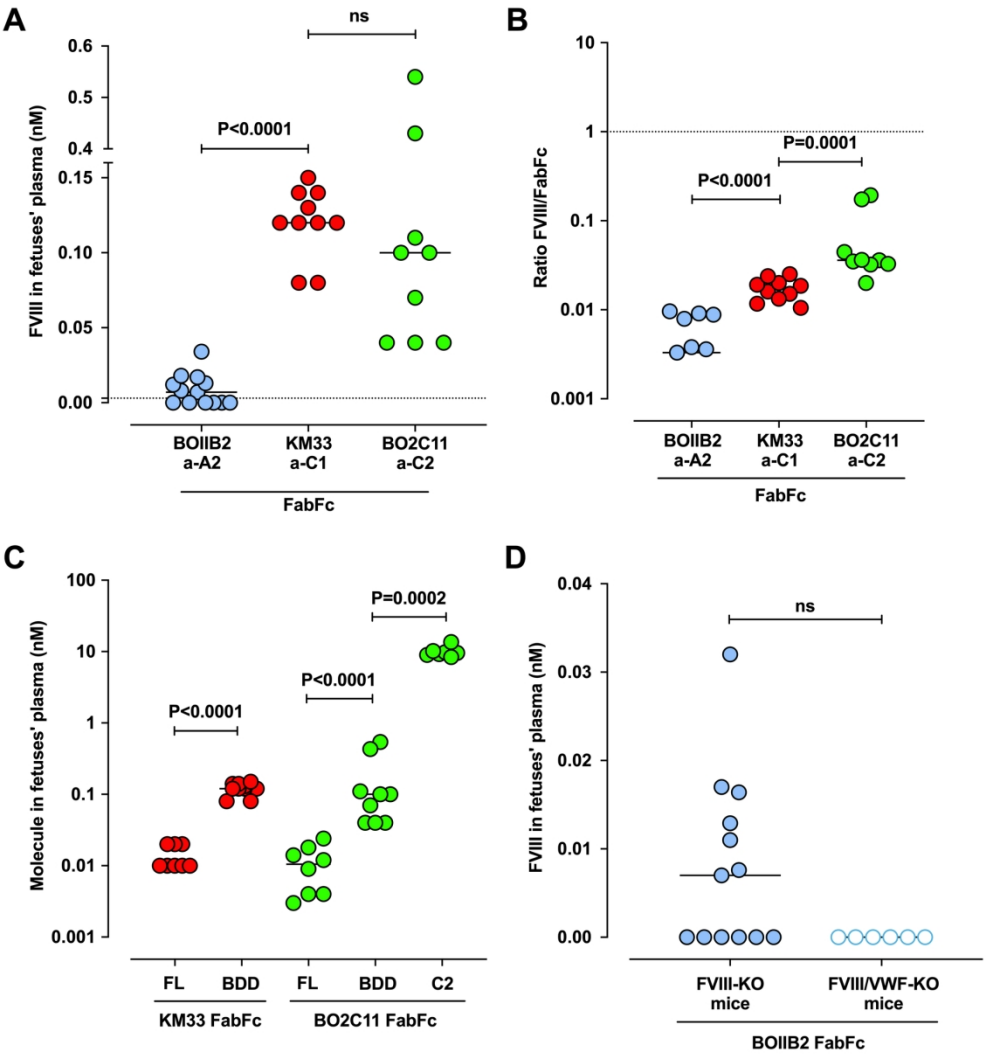

Figure 4

173x200mm (300 x 300 DPI)